

## NUMERICAL SIMULATION STUDY OF THE INCREASE IN ELECTRICAL EFFICIENCY OF THE CIGS-BASED SOLAR CELL BY SCAPS-1D

K. Madoui<sup>a</sup>, A. Ghechi<sup>b</sup>, S. Madoui<sup>c</sup>, R. Yekhle<sup>d</sup>,  D. Belfennache<sup>d\*</sup>, S. Zaiou<sup>e,f</sup>,  Mohamed A. Ali<sup>g</sup>

<sup>a</sup>Laboratory of Applied Optics, Institute of optics and precision mechanics, Ferhat ABBAS Setif-1 University, Algeria

<sup>b</sup>Laboratory of Optoelectronics and components, Institute of optics and precision mechanics. Ferhat Abbas Setif-1 University, Algeria

<sup>c</sup>Laboratory of Applied Biochemistry, University Ferhat Abbas Setif-1, 19000, Algeria

<sup>d</sup>Research Center in Industrial Technologies CRTI, P.O. Box 64, Cheraga, 16014 Algiers, Algeria

<sup>e</sup>Laboratory for Studies of Surfaces and Interfaces of Solid Materials (LESIMS), University Setif-1, 19000 Setif, Algeria

<sup>f</sup>Faculty of Natural Sciences and Life, Setif-1 University, 19000 Setif, Algeria

<sup>g</sup>School of Biotechnology, Badr University in Cairo (BUC), Badr City 11829, Cairo, Egypt

\*Corresponding Author e-mail: [belfennachedjamel@gmail.com](mailto:belfennachedjamel@gmail.com)

Received May 15, 2024; revised July 3, 2024; accepted July 12, 2024

Solar cells are currently the focus of a great deal of research. The aim is to reduce their cost price. To achieve this, we need to reduce the mass of the materials and increase the conversion efficiency of these solar cells. This has motivated research into the use of thin films such as a-Si, CdTe, CIGS. This increase in efficiency requires optimizing the performance of the photovoltaic parameters. In this modeling and simulation work, we use the SCAPS-1D software to study the effect of the recombination speed of the electrons and holes in the CIGS layer, the effect of the thickness of the layers and the effect of the gap energy of each layer of the material used for this solar cell on the short-circuit current  $J_{sc}$ , the open-circuit voltage  $V_{oc}$ , the form factor FF and the electrical efficiency  $\eta$  of the CIGS cell for a Mo/p-CIGS/p-Si/In<sub>2</sub>S<sub>3</sub>/i-ZnO/Al-ZnO single-junction structure. In this study, we found that recombination speed affects the efficiency of the photovoltaic cell. The gap energy of the absorber layers influences the cell's efficiency, while the other layers (In<sub>2</sub>S<sub>3</sub>, ZnO, Al-ZnO) do not have a great influence on solar cell performance and increasing the thickness of the absorber layer has a major influence on efficiency, increasing it up to a certain limit. The thicknesses of the CIGS, p-Si, In<sub>2</sub>S<sub>3</sub>, i-ZnO and Al-ZnO layers need to be in the order of 0.3 $\mu$ m, 0.8 $\mu$ m, 0.05 $\mu$ m, 0.07 $\mu$ m and 0.1 $\mu$ m respectively to achieve better efficiency (31.42%).

**Keywords:** Density functional theory (DFT); Binding energies; Homo-lumo energy; Fragmentation energy; Magnetic moment

**PACS:** 73.50.-h, 73.50.Pz

### 1. INTRODUCTION

The evolution and development of humanity leads to increasing energy consumption while usual energy resources decrease and pollution increases. Renewable energies appear to provide an optimal solution to address the global energy problem [1]. Among them, solar energy offers a reliable, clean and adaptable way to generate heat and electricity according to needs. More particularly, photovoltaics (PV) constitutes an “inexpensive” solution to overcome the energy supply problem of developing countries, thanks to autonomous systems making it possible not only to supply electricity but also to power systems water pumps or water filtration [2]. As part of the sustainable development approach, renewable energies make it possible to preserve planetary resources, ensure the security and diversity of energy supplies and reduce the environmental impact of our energy consumption. The PV market today is essentially based on silicon technology [3]. Currently, the sector is largely dominated by crystalline silicon technology with nearly 93% of global production. However, the production of silicon-based solar cells remains expensive and requires a large quantity of material [4]. In addition, silicon cells currently have a maximum efficiency of 25.6% in the laboratory, which is very close to the maximum theoretical limit for a single junction cell [5]. Consequently, the growing need for photovoltaic energy has pushed research into the use of other alternative materials, although this in no way means an end to research in the silicon sector [6-8]. Research, very numerous and varied, focuses mainly on thin film technologies [9-12]. CIGS-based thin-film solar cells were developed by Arco in the late 1980s using a two-step process with Cu and In as metal precursors, followed by reactive annealing in an H<sub>2</sub>S atmosphere, during of which the absorbing layer (CIGS) is doped with N/A. Since then, the leading research organization in the field of CIGS solar cells (NREL) has reported the remarkable improvements in efficiency achieved by these cells deposited on substrates of rigid glass [13-16]. The most promising second generation materials are amorphous and microcrystalline silicon, cadmium tellurium (CdTe) and the Cu (In<sub>x</sub>, Ga<sub>1-x</sub>)(S<sub>y</sub>,Se<sub>1-y</sub>)<sub>2</sub> (CIGSSe) family of chalcopyrites. These materials are used in the form of a thin layer deposited on a substrate (soda glass, ceramic, polyamide, etc.), which not only reduces the costs of the final module, but also expands the range of applications of the cells solar. In a few years, the efficiency of solar cells based on Cu(In,Ga)Se<sub>2</sub> (CIGS) increased from 20.8% [13] to 22.6% [14]. Many studies have proven that cadmium tablets have enabled high productivity, but they nevertheless tend to be replaced, due to their toxicity, by cadmium-free, higher bandgap materials (In<sub>2</sub>Se<sub>3</sub>, ZnS, Zn(S,O), Zn(S,O,OH), (Zn,Mg) O) to reduce optical losses [17-20].

Whatever the structure of a solar cell, its parameters need to be optimized. Typically, the parameters to be optimized are the  $E_g$  bandgap thicknesses and widths, and the doping levels of the various layers making up the cell. Solar cell optimization therefore involves studying the influence of these parameters on efficiency, in order to obtain a structure that delivers maximum efficiency. This optimization can be carried out either experimentally or by simulation. Experimental optimization has the advantage of being real, but it is tedious, boring and expensive. What's more, we don't have access to certain cell parameters. Simulation-based optimization, on the other hand, follows a mathematical model of the real system. In this work, we will use SCAPS-1. This allows us to understand in detail the functioning of the structure of thin film solar cells and the main physical phenomena which govern the operation of our devices by carefully taking into account: the short circuit current  $J_{sc}$ , the open circuit voltage  $V_{oc}$ , efficiency ( $\eta\%$ ) and filling factor (FF) [21] CIGS, a non-toxic material widely available on Earth, knowing that it is expensive. To reduce the thickness of CIGS, we choose the following solar cell structure: Al-ZnO/i-ZnO/ $In_2S_3$ /p-CIGS/p-Si. CIGS and Si we will use as absorbing layers and  $In_2S_3$  as insulating layer. We study the performance of CIGS-based solar cells by changing the spacing energy and thickness of each cell layer.

### 2. OVERVIEW OF SCAPS-1D SOFTWARE

SCAPS (solar cell capacitance simulator) is a one-dimensional solar cell simulation program developed at the Department of Electronics and Information Systems (ELIS) at Ghent University, Belgium. Several researchers have contributed to its development: Alex Niemegeers, Marc Burgelman, Koen Decock, Stefaan Degraeve, Johan Verschraegen. The program was initially developed for cellular structures of the  $CuInSe_2$  and  $CdTe$  family. Recent developments now make the program equally applicable to crystalline solar cells (Si and GaAs family) and amorphous cells (a-Si and micromorphous Si). The latest version, SCAPS 3.10, may 2020. The program runs on PCs running Windows 95, 98, NT, 2000, XP, Vista, Windows 7,8 and 10, and takes up around 50 MB of space. It is freely accessible to the PV research community (universities and research institutes, companies) [22-27].

### 3. PRESENTATION OF THE STUDIED CELL

The difficulty in simulating electronic devices lies in the choice of simulation parameters. For this, we took a work submitted by Mohottige RN and Kalawila SP, they found an electrical efficiency of ~26% [28]. The solar cell architecture simulated in this study had a substrate/Mo/p-Si/pCIGS/n- $In_2S_3$ /i-ZnO/Al-ZnO/metal grid, as shown in Fig. (1).

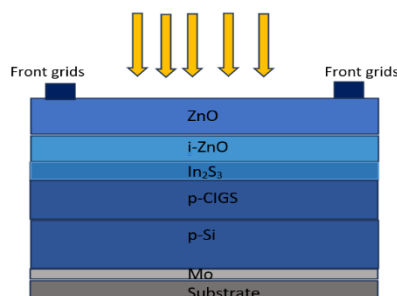


Figure 1. Schematic diagram of the CIGS Structure [28].

The defect density was implemented in the P-Si, CIGS and  $In_2S_3$  layers. The i-ZnO insulating layer improves the performance of thin-film solar cells. This material can fill the pinholes in the structure and reduce the electric short circuit [29]. Electrical short-circuiting of devices is a key concern during the manufacturing process, and it's an excellent solution to suppress between interfaces to increase efficiency. So, the i-ZnO layer acts as an electron backscatter barrier, improving  $J_{sc}$  and efficiency. Table 1, shows the optimized material properties for each layer used in the simulation. These parameters are entered into the SCAPS software.

Table 1. Material parameters used in the simulation [28]

Parameters	CIGS	P- Si	$In_2S_3$	I-Zno	Al-Zno
Thicknesses (nm)	100 1000	1000	50	70	100
Gap strip (ev)	1.100	1.120	2.800	3.300	3.300
Electronic affinity (ev)	4.500	4.500	4.700	4.600	4.600
Relative Permittivity	13.600	11.900	13.500	9.000	9.000
CB ( $1/cm^3$ )	2.200E +18	2.800E +19	1.800E +18	2.200E +18	2.200E +18
VB( $1/cm^3$ )	1.800E +19	2.650E +19	4.000E +13	1.800E +19	1.800E +19
Electron mobility ( $cm^2/Vs$ )	1.000E +2	1.450E +3	4.000E +2	1.000E +2	1.000E +2
Hole mobility ( $cm^2/Vs$ )	2.500E +1	5.000E +2	2.100E +2	2.500E +1	2.500E +1
ND( $1/cm^3$ )	0.000E +0	0.000E +0	1.000E +18	1.000E +16	1.000E +18
NA( $1/cm^3$ )	2.000E +16	1.000E +20	1.000E +1	0.000E +0	0.000E +0
Defect density ( $1/cm^3$ )	1.000E +14	1.000E +14	1.000E +14	0.000E +0	0.000E +0

This digital survey was carried out in three stages: The effect of the recombination rate of electrons and holes on the cell was studied. Next, we studied the influence of varying the gap energy values of each layer on the cell's

performance, and extracted the relationship between the gap energy of the CIGS and p-Si absorber layers. Finally, cell performance was optimized by changing the thicknesses of each cell layer: the CIGS and P-Si absorber layers, the  $\text{In}_2\text{S}_3$  buffer layer, the i-ZnO insulator layer and the Al-ZnO window layer. The simulation was carried out under solar spectrum AM 1.5 and at an incident power of  $p = 1000\text{Wm}^{-2}$ . SCAPS simulation can perform measurements under light and dark conditions and in various temperature ranges and other parameters. In this study, we maintained the thickness of the p-Si, i-ZnO and Al-ZnO layers at 1  $\mu\text{m}$ , 50 nm and 100 nm respectively [28] in order to investigate solar cell parameters such as: Short-circuit current  $J_{sc}$ , Open-circuit voltage  $V_{oc}$ , Efficiency ( $\eta\%$ ) and fill factor (FF). The first layer deposited on the substrate is the back contact electrode. Its main role is to collect the charges generated in the cell. From an electrical point of view, it constitutes the positive pole of the photovoltaic generator. This layer is composed of Molybdenum (Mo) and is between 50 nm and 1500 nm thick, this result is consistent with the results reported in the literature [30,31]. In addition, the Mo layer is used as a reflector to lengthen the optical path of light in the CIGS, thereby increasing the number of photons absorbed [32]. Numerous studies have also proven that during the deposition of CIGS on Mo, a thin layer of MoSe2 is formed at the interface. This layer is responsible for establishing ohmic contact with the CIGS [33,34].

#### 4. EFFECT OF THE RECOMBINATION SPEED OF ELECTRONS AND HOLES

Generation in semiconductors is the process in which electron-hole pairs are created. The energy necessary for the transition of an electron from the valence band to the conduction band is obtained by different physical processes: thermal absorption, external electric field and absorption of photons by the semiconductor. The electron-hole pairs created are sooner or later recombined. In this section, we will present in a first part the results relating to the effect of the recombination speed for a CIGS thickness of  $0.1\mu\text{m}$ : as well as their analyzes in order to understand the effect of the recombination speed of electrons and holes. In a second part, Effect of the recombination rate for a CIGS thickness of  $0.3\mu\text{m}$  will be presented so that it can be examined and properly interpreted and this in comparison with the conclusions resulting from the electron recombination rate and we fix the hole rate. To do this, different parameters such as: the thicknesses of each layer of the Al-ZnO/i-ZnO/ $\text{In}_2\text{S}_3$ /p-CIGS/p-Si solar cell will be varied, to obtain the best electrical efficiency.

##### 4.1. Effect of recombination speed for a cigs thickness of $0.1\mu\text{m}$

###### 4.1.1. Effect of electron recombination speed

The values of the electron surface recombination velocity are varied, and the hole velocity is fixed. The results obtained are shown in Table 2.

**Table 2.** Functional parameters of the solar cell with different electron surface recombination velocities.

Electron recombination speed (cm/s)	Recombination speed of holes (cm/s)	$V_{oc}$ (V)	$J_{sc}$ (mA/cm <sup>2</sup> )	FF (%)	$\eta$ (%)
8.00E 0	1.00E 7	0.801	38.96	83.38	26.03
9.00E 0	1.00E 7	0.800	38.95	83.45	26.02
1.00E 1	1.00E 7	0.7996	38.94	83.51	26.12
1.00E 2	1.00E 7	0.781	38.44	84.20	25.29
1.20E 2	1.00E 7	0.779	38.36	84.17	25.18
1.70E 2	1.00E 7	0.777	38.19	84.13	24.98
1.90E 2	1.00E 7	0.776	38.14	84.11	24.91
1.00E 3	1.00E 7	0.768	37.37	83.58	24.01
1.00E 4	1.00E 7	0.766	37.00	83.28	23.60
1.00E 5	1.00E 7	0.765	36.95	83.24	23.55
1.00E 6	1.00E 7	0.765	36.95	83.23	23.55
1.00E 7	1.00E 7	0.765	36.95	83.23	23.55
1.00E 8	1.00E 7	0.765	36.95	83.23	23.55

According to the results listed in the Table (2), we can summarize them in the following points :

- For an electronic recombination speed equal to  $1.2 \times 10^2$  cm/s, the efficiency is equal (25.18%). This results is in agreement with those reported in the literature [28]
- For electron recombination velocity equal to 10 cm/s, we obtain an electrical efficiency (26.12%) better than that found in the Ref [28].
- For electron recombination values below or above 10 cm/s, we find a decrease in electrical efficiency.

Based on these remarks, we have chosen the electron recombination speed 10 cm/s for an optimum electrical efficiency value ( $\eta=26.12\%$ ).

###### 4.1.2. Effect of hole recombination speed

Fixing the electron recombination speed at 10 cm/s and varying the surface recombination speed of the holes, the results found are shown in Table 3.

**Table 3.** Functional parameters of the solar cell with different surface recombination rates

Electron recombination speed (cm/s)	Recombination speed of holes (cm/s)	$V_{oc}$ (V)	$J_{sc}$ (mA/cm <sup>2</sup> )	FF (%)	$\eta$ (%)
1.00E 1	1.00E 0	0.8004	39.52	77.95	24.55
1.00E 1	8.00E 0	0.806	39.26	80.98	25.63
1.00E 1	9.00E 0	0.806	39.24	81.11	25.67
1.00E 1	1.00E 1	0.8066	39.23	81.23	25.70
1.00E 1	1.00E 2	0.8089	39.05	82.49	26.06
1.00E 1	1.20E 2	0.8089	39.04	82.52	26.07
1.00E 1	1.70E 2	0.8090	39.039	82.58	26.08
1.00E 1	1.90E 2	0.8091	39.037	82.59	26.08
1.00E 1	1.00E 3	0.8092	39.022	82.68	26.11
1.00E 1	1.00E 4	0.8093	39.01	82.70	26.11
1.00E 1	1.00E 5	0.8093	39.019	82.70	26.12
1.00E 1	1.00E 6	0.8093	39.019	82.70	26.12
1.00E 1	1.00E 7	0.8093	39.019	82.70	26.12
1.00E 1	1.00E 8	0.8093	39.019	82.70	26.12
1.00E 1	1.00E 9	0.8093	39.019	82.70	26.12

It can be seen that increasing the surface recombination speed of the holes increases the electrical efficiency to a certain value, after which it remains constant. For a hole recombination speed equal to 10 cm/s, we obtain a higher efficiency (26.12%). We can see that the backside recombination velocities for electrons and holes influence solar cell efficiency. Based on the results obtained, our choice is based on an electron speed of 10 cm/s and a hole speed of  $1 \cdot 10^7$  cm/s.

#### 4.2. Effect of recombination rate for a cigs thickness of 0.3 $\mu$ m

The thicknesses of each layer of the Al-ZnO/i-ZnO/In<sub>2</sub>S<sub>3</sub>/p-CIGS/p-Si solar cell chose respectively 100nm, 70nm, 50 nm, 0.3  $\mu$ m and 1  $\mu$ m, to achieve the best electrical efficiency [28]. We vary the values of the electron surface recombination rate, and fix the hole rate, and then do the reverse, fix the value of the electron surface recombination rate that gives the best electrical efficiency, and vary the hole surface recombination rate. The results obtained are shown in Tables 4 and 5.

**Table 4.** Functional parameters of the solar cell with different surface electron recombination speed for CIGS layer thickness = 0.3  $\mu$ m

Electron recombination speed (cm/s)	Recombination speed of holes (cm/s)	$V_{oc}$ (V)	$J_{sc}$ (mA/cm <sup>2</sup> )	FF (%)	$\eta$ (%)
1.00E 0	1.00E 7	0.7749	37.617	83.54	24.34
8.00E 0	1.00E 7	0.7746	37.616	83.54	24.34
9.00E 0	1.00E 7	0.7746	37.626	83.53	24.35
1.00E 1	1.00E 7	0.7746	37.615	83.55	24.34
1.00E 2	1.00E 7	0.7722	37.520	83.63	24.23
1.20E 2	1.00E 7	0.7719	37.502	83.63	24.21
1.70E 2	1.00E 7	0.7712	37.460	83.64	24.16
1.90E 2	1.00E 7	0.7710	37.445	83.64	23.14
1.00E 3	1.00E 7	0.7678	37.134	83.48	23.80
1.00E 4	1.00E 7	0.7659	36.849	83.28	23.50
1.00E 5	1.00E 7	0.7656	36.801	83.24	23.45
1.00E 6	1.00E 7	0.7655	36.7960	83.23	23.45
1.00E 7	1.00E 7	0.7655	36.7955	83.23	23.45
1.00E 8	1.00E 7	0.7655	36.7954	83.23	23.45

**Table 5.** Functional parameters of the solar cell with different surface recombination rates of the holes for a CIGS layer thickness = 0.3  $\mu$ m

Electron recombination speed (cm/s)	Recombination speed of holes (cm/s)	$V_{oc}$ (V)	$J_{sc}$ (mA/cm <sup>2</sup> )	FF (%)	$\eta$ (%)
1.00E 0	1.00E 0	0.7738	37.680047	76.66	22.35
1.00E 0	8.00E 0	0.7753	37.661992	81.09	23.68
1.00E 0	9.00E 0	0.7753	37.66006	81.27	23.73
1.00E 0	1.00E 1	0.7753	37.65832	81.43	23.77
1.00E 0	1.00E 2	0.7753	37.63201	83.23	24.27
1.00E 0	1.20E 2	0.7753	37.631144	83.28	24.27
1.00E 0	1.70E 2	0.7753	37.629822	83.35	24.29
1.00E 0	1.90E 2	0.7753	37.629479	83.37	24.31
1.00E 0	1.00E 3	0.7753	37.627015	83.50	24.31
1.00E 0	1.00E 4	0.7753	37.626470	83.52	24.35
1.00E 0	1.00E 5	0.7753	37.626416	83.53	24.35

Electron recombination speed (cm/s)	Recombination speed of holes (cm/s)	$V_{oc}$ (V)	$J_{sc}$ (mA/cm <sup>2</sup> )	FF (%)	$\eta$ (%)
1.00E 0	1.00E 6	0.7753	37.626410	83.53	24.35
1.00E 0	1.00E 7	0.7753	37.626410	83.53	24.35
1.00E 0	1.00E 8	0.7753	37.626409	83.53	24.35
1.00E 0	1.00E 9	0.7753	37.626409	83.53	24.35

From this study, we can say that to obtain the best electrical efficiency from the cell, it is only necessary to vary the electron recombination rate. For a CIGS thickness of 0.1  $\mu\text{m}$ , the cell gives a high efficiency compared with a thickness of 0.3  $\mu\text{m}$ . A major drawback of practical devices is the reduction in CIGS layer thickness due to interlayer mixing and aging. Thickness reduction allows electronic recombination with the back contact.

### 4.3. Effect of varying the gap energy of solar cell layers

#### 4.3.1. Effect of Varying the Gap Energy of The Cigs Layer

The variation in the gap energy values induces a modification of the photovoltaic parameters of the cell. The effects of the gap energy variation on the different photovoltaic parameters of the cell are illustrated in Fig. (2).

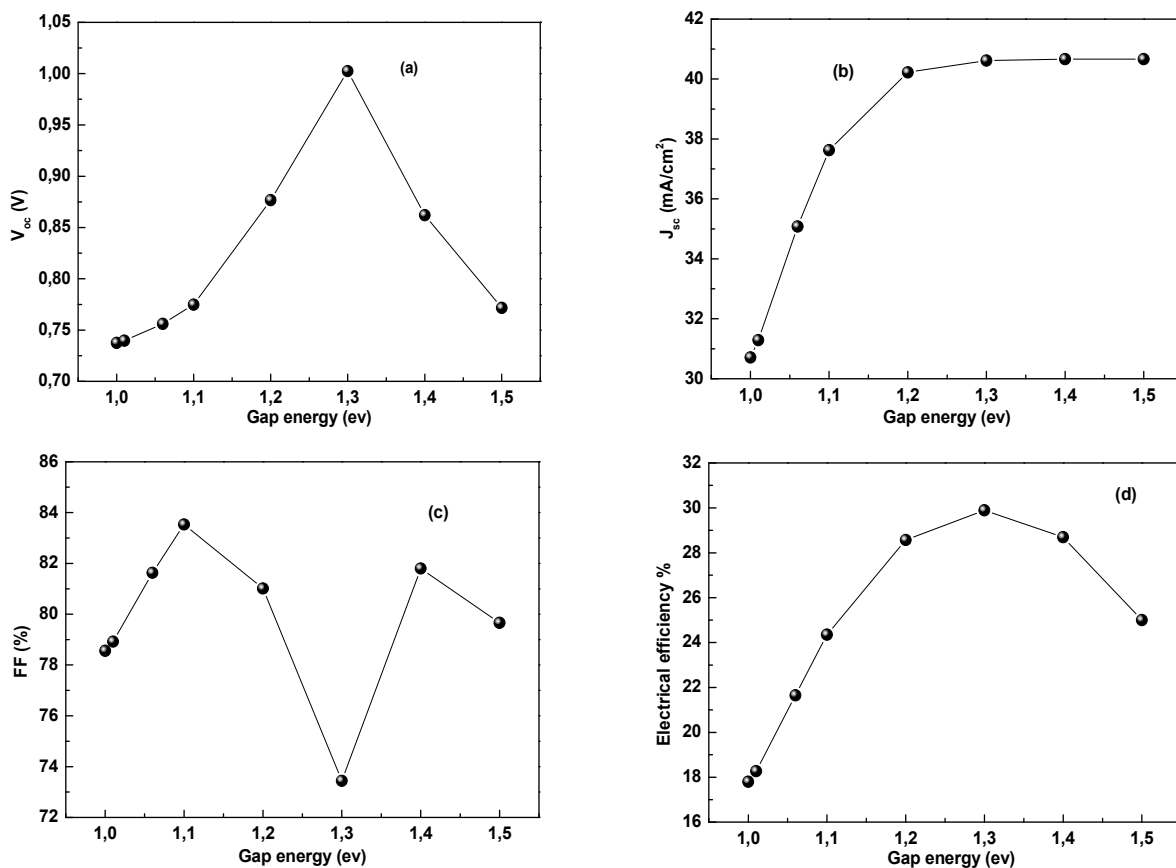


**Figure 2.** Effect of varying the gap energy of the CIGS absorber layer of the CIGS cell on: a) The open-circuit voltage  $V_{oc}$ , b) The short-circuit voltage density circuit  $J_{sc}$ , c) Form factor FF%, d) Efficiency  $\eta$ %

The observation to draw from this figure is that when the gap energy of the CIGS has a value of 1.3 eV, the best efficiency is obtained. However, when we increase the spacing energy of the CIGS absorbing layer from 1 eV to 1.5 eV, we notice that:

- The short circuit current density ( $J_{sc}$ ) increases from 37.626 mA/cm<sup>2</sup> to 40.662mA/cm<sup>2</sup>.
- Open circuit voltage ( $V_{oc}$ ) increases from 0.775 V to 1.002 V then decreases to 0.771 V.
- Form factor (FF%) increases and decreases randomly from 73.44% to 83.53%.
- The yield ( $\eta$ ) increases from 24.35% to 29.89%, then decreases to 25.00%.

#### 4.3.2. Effect of Varying the Gap Energy of The Si Layer

The various values of the gap energy of the SI absorber layer, ranging from 1 eV to 1.12 eV, influence the photovoltaic parameters of the cell, as shown in Fig (3).

From the results, we can see that when the gap energy has a value of 1eV, the best performance is achieved. When we increase the gap energy values of the p-Si absorber layer from 1 eV to 1.12 eV, we notice that:

- The short-circuit current density ( $J_{sc}$ ) decreases from  $45.424 \text{ mA/cm}^2$  to  $40.615 \text{ mA/cm}^2$ .
- Open-circuit voltage ( $V_{oc}$ ) increases from  $0.7963 \text{ V}$  to  $1.002 \text{ V}$
- Form factor (FF%) decreases from  $86.40\%$  to  $73.44\%$ .
- Electrical efficiency ( $\eta$ ) decreases from  $31.25\%$  to  $29.48\%$ , then increases to  $29.89\%$ .

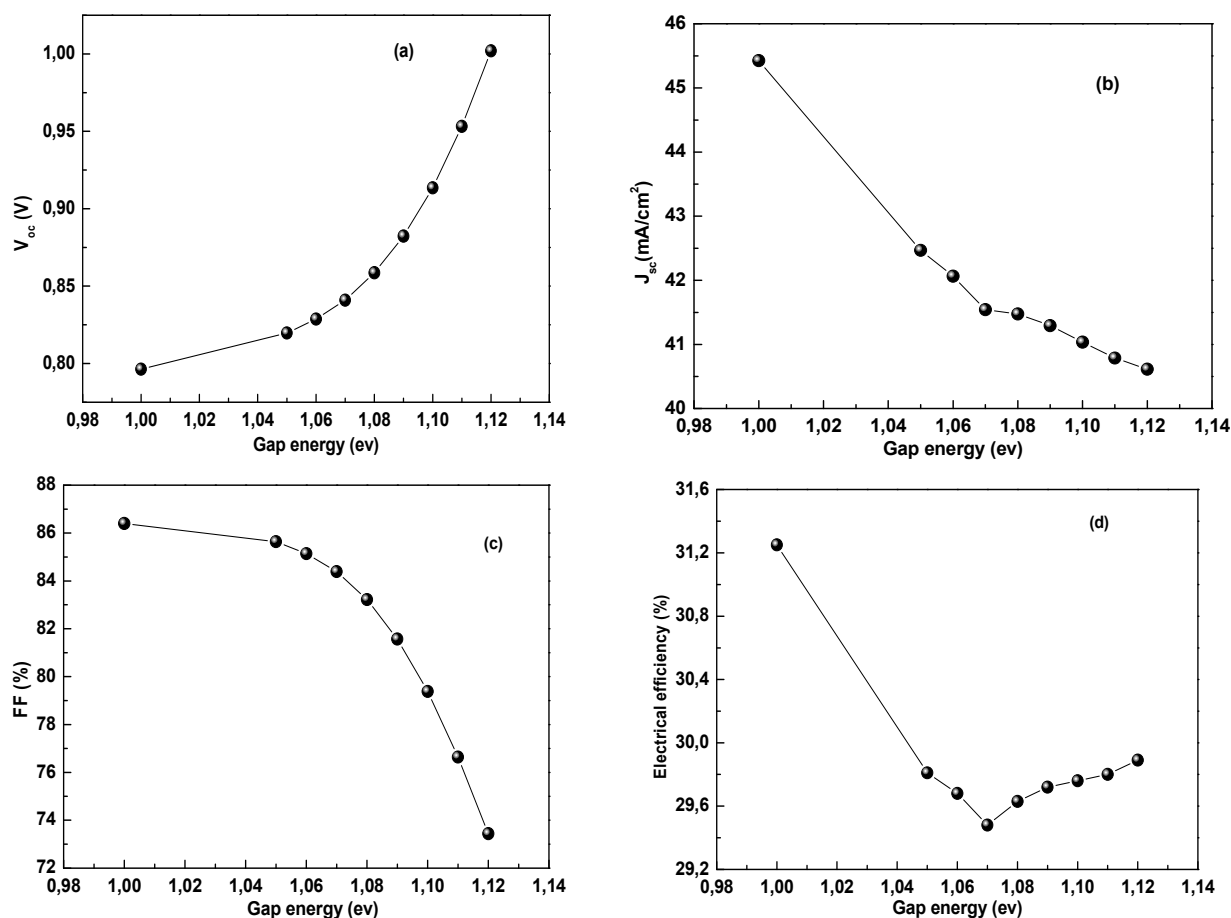


**Figure 3.** Effect of the gap energy of the Si absorber layer of the CIGS cell on: a) Open-circuit voltage  $V_{oc}$ , b) Short-circuit voltage density  $J_{sc}$ , c) Form factor FF%, d) Efficiency  $\eta$

#### 4.3.3. Effect of Varying the Gap Energy of The $\text{In}_2\text{S}_3$ Buffer Layer

The optical gap energy of  $\text{In}_2\text{S}_3$  is  $2.56 \text{ eV}$ . We chose to vary the gap energy between  $2 \text{ eV}$  and  $2.8 \text{ eV}$ . These different values, which influence the photovoltaic parameters of the cell, are given in Fig (4).

From the results shown in the Fig. 4, we note that the variation in  $\text{In}_2\text{S}_3$  gap energy values has no influence on the cell's photovoltaic parameters.

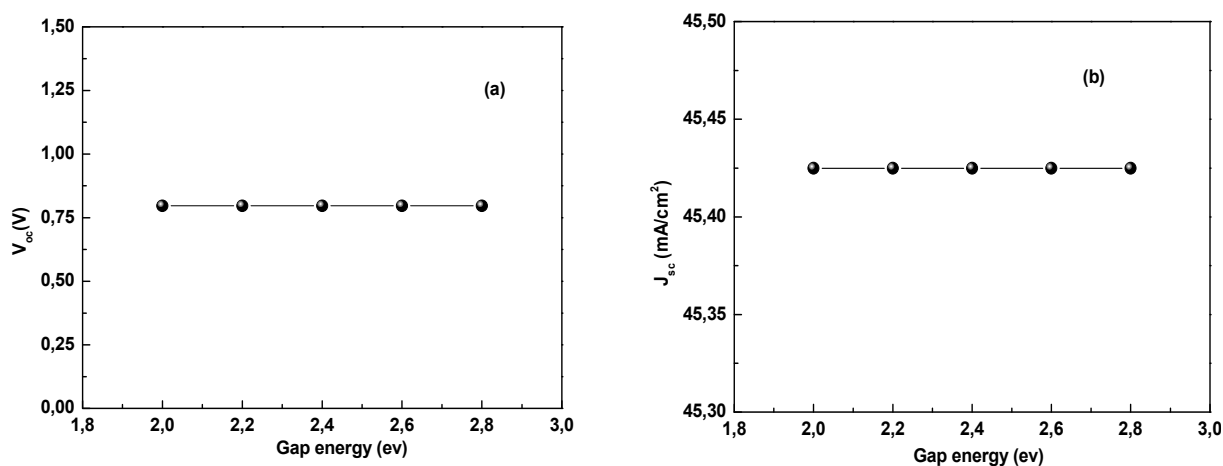


**Figure 4.** Effect of varying the gap energy of the  $\text{In}_2\text{S}_3$  buffer layer a) the open-circuit voltage  $V_{oc}$ , b) short-circuit voltage density  $J_{sc}$ , c) form factor FF%, d) efficiency  $\eta$  %.

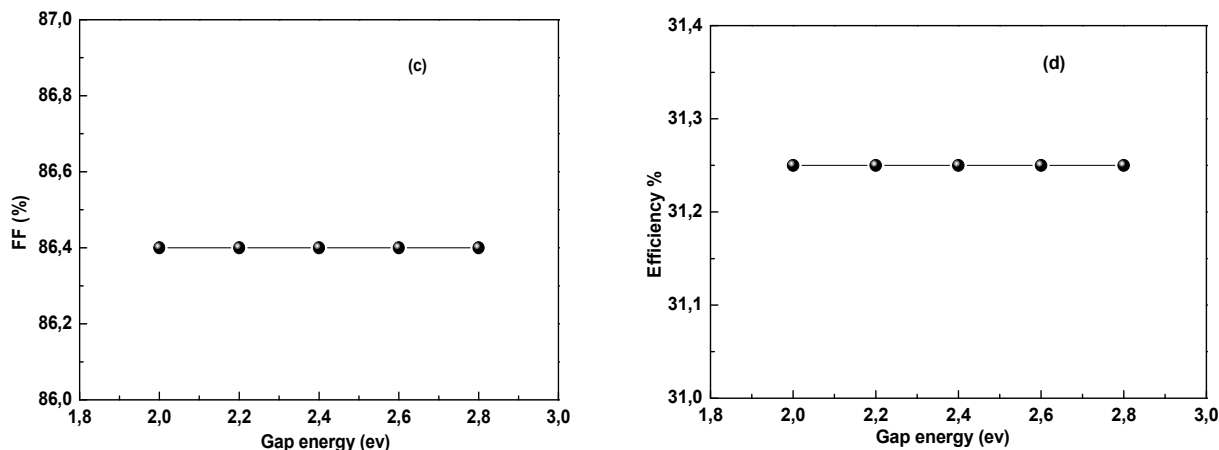


**Figure 4 (continuation).** Effect of varying the gap energy of the the In<sub>2</sub>S<sub>3</sub> buffer layer  
 a) the open-circuit voltage  $V_{oc}$ , b) short-circuit voltage density  $J_{sc}$ , c) form factor FF%, d) efficiency  $\eta$  %

#### 4.3.4. Effect of Varying the Gap Energy of the ZNO Layer

Fig. 5 shows the different values of ZnO gap energy, ranging from 3.2 eV to 3.45 eV, which influence the photovoltaic parameters of the cell.

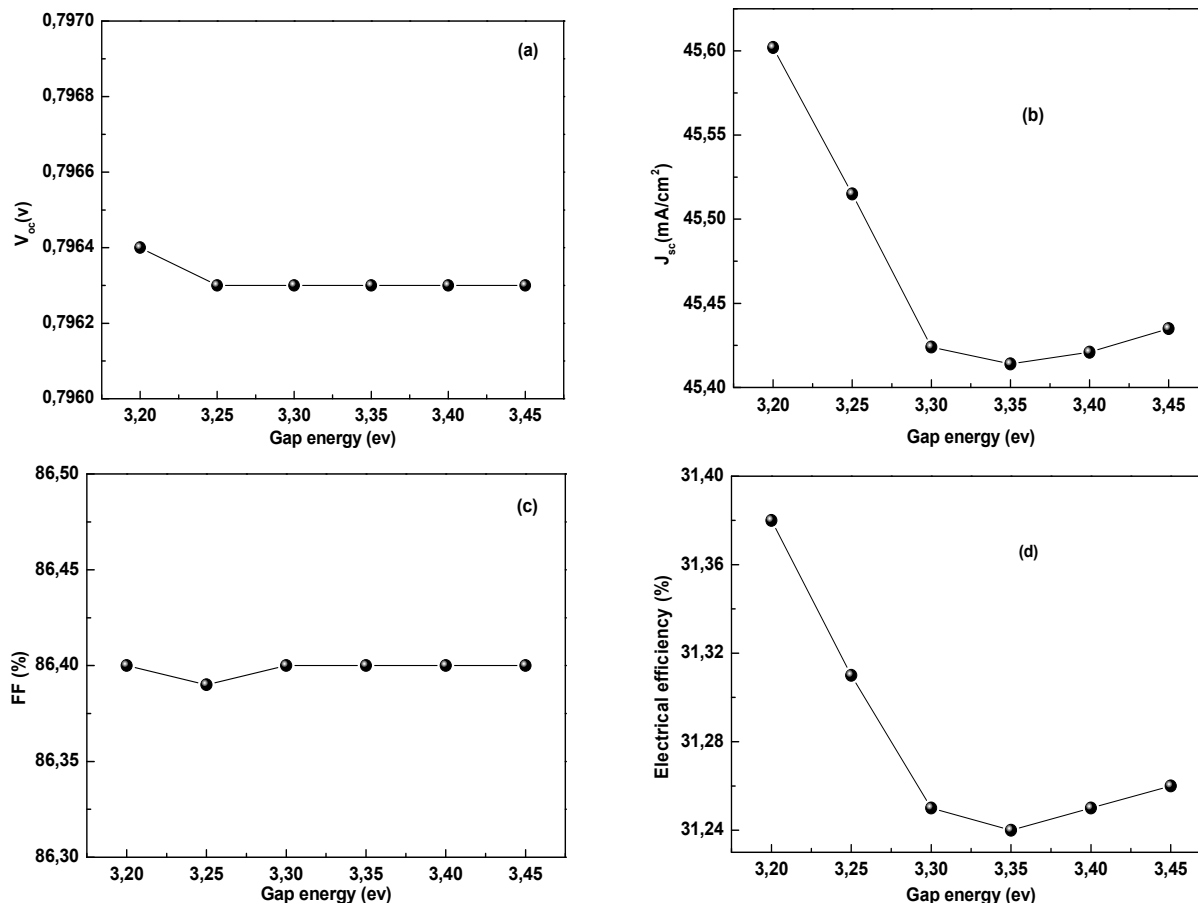


**Figure 5.** Effect of varying the gap energy of the ZnO layer  
 a) the open-circuit voltage  $V_{oc}$ , b) short-circuit voltage density  $J_{sc}$ , c) form factor FF%, d) efficiency  $\eta$  %

We note that varying ZnO gap energy values do not influence open-circuit voltage  $V_{oc}$  and form factor FF, but do influence short-circuit voltage density  $J_{sc}$ . The best electrical efficiency is obtained when the ZnO gap energy reaches 3.2 eV.

#### 4.3.5. Effect of Varying the Gap Energy of the Al-ZnO Layer

The different values of the Al-ZnO gap energy, ranging from 3.2 eV to 3.45 eV, which influence the photovoltaic parameters of the cell, are given in Fig. 6.

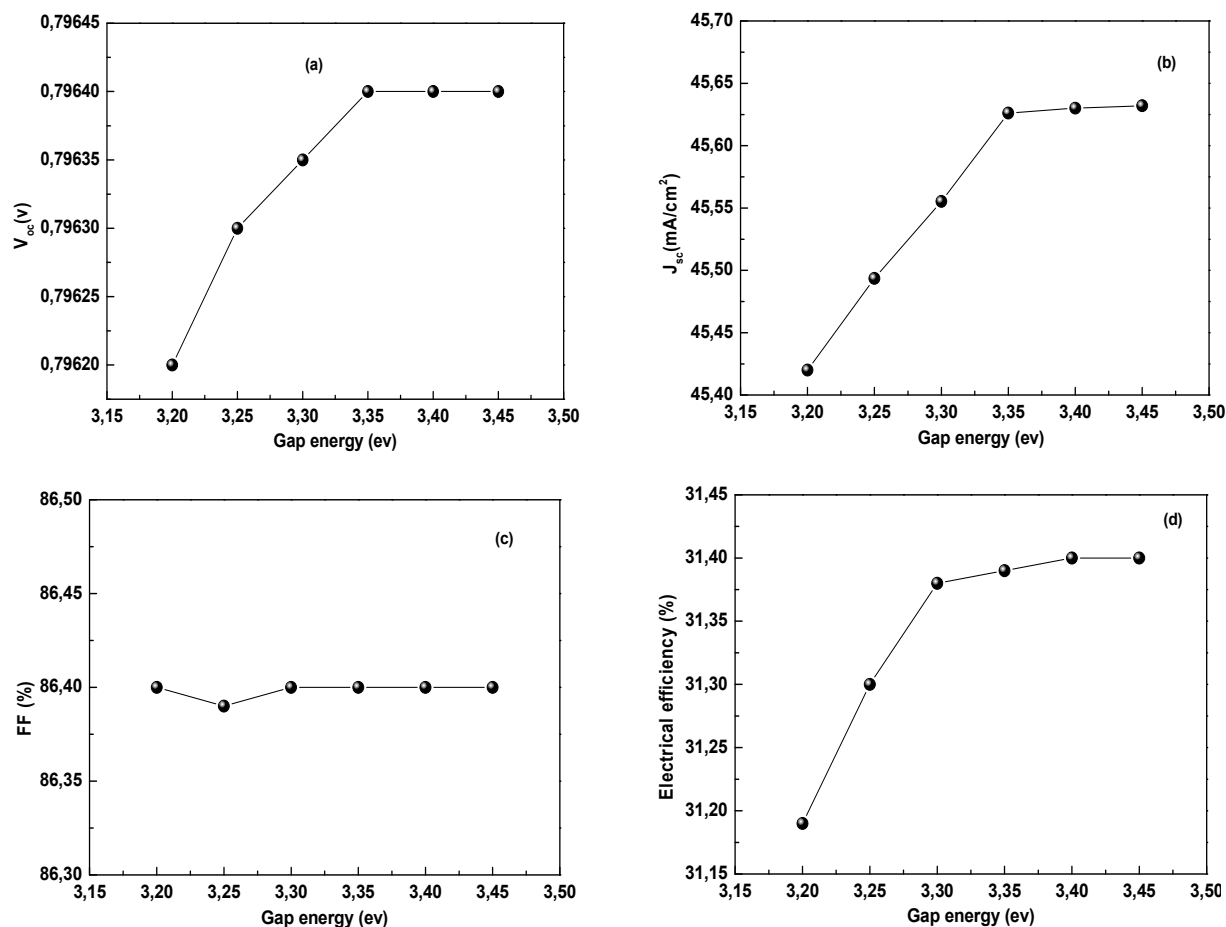


**Figure 6.** Effect of varying the gap energy of the AL-ZnO layer  
a) the open-circuit voltage  $V_{oc}$ , b) short-circuit voltage density  $J_{sc}$ , c) form factor FF%, d) efficiency  $\eta\%$

We note that varying Al-ZnO gap energy values have no influence on open-circuit voltage  $V_{oc}$  and form factor FF, but there is a small influence on short-circuit voltage density  $J_{sc}$ . The best electrical performance is obtained when the gap energy of Al-ZnO reaches 3.4 eV. The results found for Al-ZnO are similar to those found for ZnO. So, we can say that the gap energy of the absorber layers influences the cell's efficiency, while the other layers ( $\text{In}_2\text{S}_3$ , ZnO, Al-ZnO) do not have a great influence. This result is in good agreement with those reported in the literatures [35].

#### 4.4. The Effect of Thickness Variation:

##### 4.4.1. Cigs Thickness

The effect of varying the thickness of the CIGS absorber layer (from 0.1  $\mu\text{m}$  to 1  $\mu\text{m}$ ) on cell performance was simulated. The simulated,  $V_{oc}$ ,  $J_{sc}$ , FF and  $\eta$  (efficiency) curves are shown in Fig. (7).

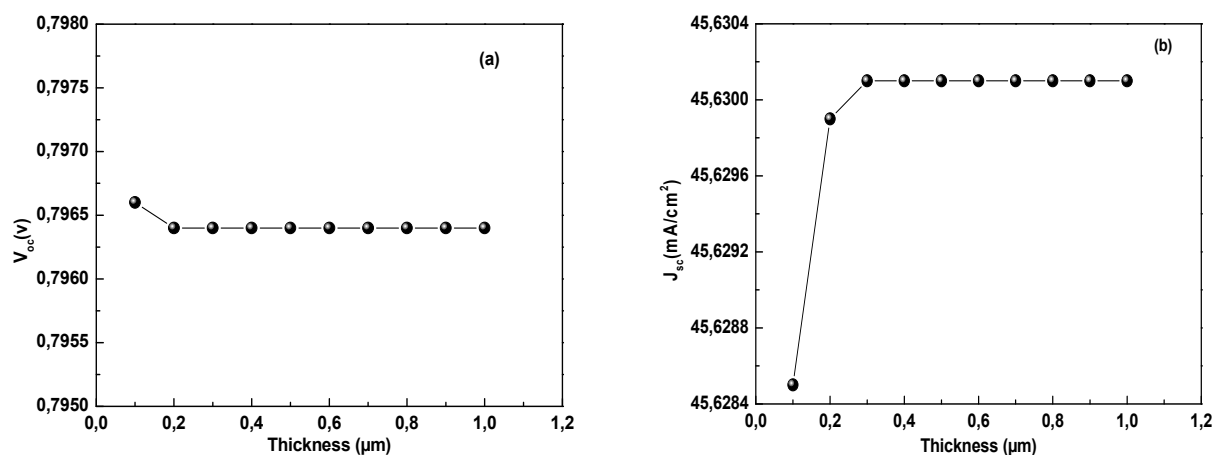


**Figure 7.** Effect of CIGS thickness on a) the open-circuit voltage  $V_{oc}$ ,  
b) short-circuit voltage density  $J_{sc}$ , c) form factor FF%, d) efficiency  $\eta\%$



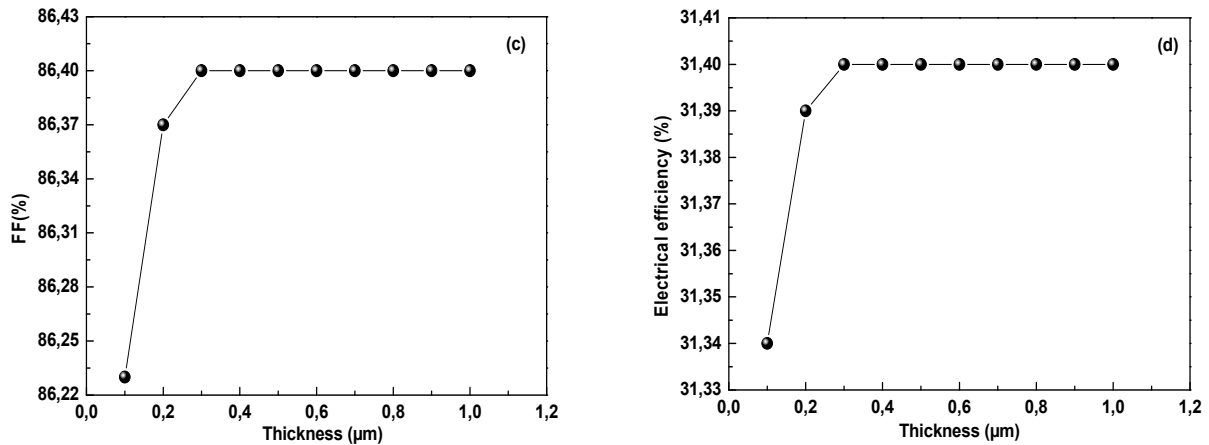


**Figure 7(continuation).** Effect of CIGS thickness on a) the open-circuit voltage  $V_{oc}$ , b) short-circuit voltage density  $J_{sc}$ , c) form factor FF%, d) efficiency  $\eta$  %

According to the results obtained, the CIGS layer thickness that gives the highest efficiency is 0.3 μm. The variation in CIGS layer thickness, between 0.1 μm and 1 μm, has little effect on short-circuit current density ( $J_{sc}$ ), open-circuit voltage ( $V_{oc}$ ), form factor (FF%) and efficiency ( $\eta$ ). Indeed, when the thickness of the CIGS layer is 0.3 μm, so the total thickness of the absorbing layer (CIGS+ p-Si) will be 1.3 μm, leads to an increase in cell performance and in particular efficiency.

#### 4.4.2. Absorbent Layer Thickness P-Si

Many researchers have worked to consolidate the photovoltaic potential offered by the thin-film p-Si sector [36-38]. As a result, they recorded an improvement in electronic properties. In this simulation step, the thickness of the CIGS layer is set at 0.3 μm. The different p-Si thicknesses, ranging from 0.3 μm to 1.3 μm, influence the photovoltaic parameters of the cell and are given in Fig. (8).

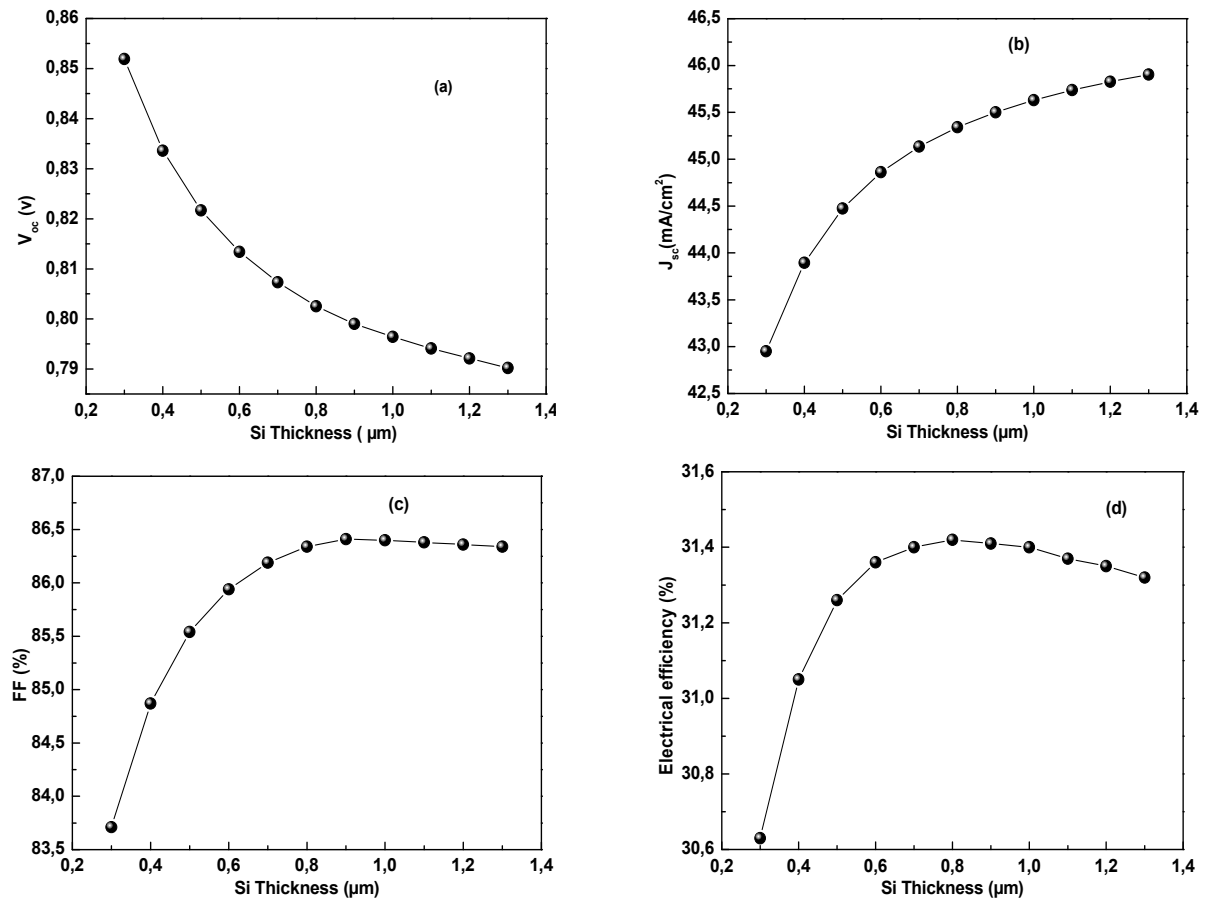


**Figure 8.** Effect of Si thickness on: a) The open-circuit voltage  $V_{oc}$ , b) The short-circuit current density  $J_{sc}$ , c) The form factor FF%, d) Efficiency  $\eta$  %

According to the results obtained, the 0.8  $\mu\text{m}$ -thick p-Si absorber layer gives a better performance. It can be seen that there is a threshold thickness (0.8  $\mu\text{m}$ ) for both form factor (FF) and efficiency ( $\eta$ ) to be high, and above or below this thickness value there is a decrease in these parameters. And we also notice that increasing thickness leads to an increase in short-circuit current density ( $J_{sc}$ ) and a decrease in open-circuit voltage ( $V_{oc}$ ). In fact, to achieve good efficiency (31.42%), the thickness of the absorber layer (CIGS+ p-Si) must be equal to 1.1  $\mu\text{m}$ , because at this thickness there is a maximum generation of electron-hole pairs and a decrease in contact return recombination.

#### 4.4.3. $\text{In}_2\text{S}_3$ Buffer Layer Thickness

Most CIGS-based ultra-thin solar cells incorporate a buffer layer to improve efficiency and other solar cell parameters. The central role of the buffer layer is to prevent unwanted bypass paths and protect the injection region during manufacturing. We set the thickness of the combined absorber layer (CIGS + p-Si) at 1.1  $\mu\text{m}$  and then varied the thickness of the  $\text{In}_2\text{S}_3$  buffer layer (from 20 nm to 100 nm). The results obtained are shown in Fig (9). From the results obtained, it can be seen that the effect of varying the thickness of the buffer layer does not greatly influence cell performance. It can be seen that increasing the thickness will decrease the efficiency and the short-circuit current density  $J_{sc}$ .

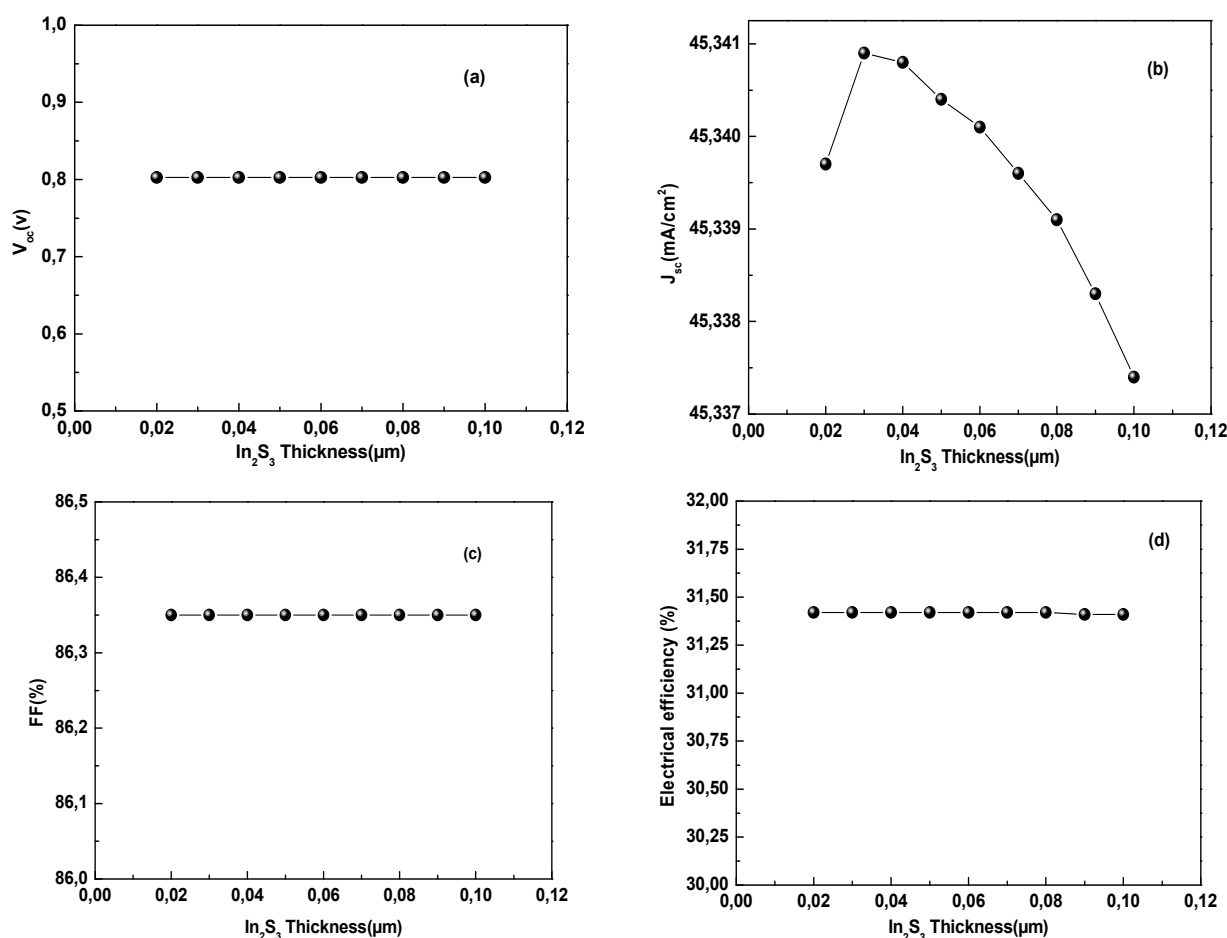


**Figure 9.** Effect of varying  $\text{In}_2\text{S}_3$  thickness on: a) Open-circuit voltage  $V_{oc}$ , b) Short-circuit current density  $J_{sc}$ , c) Form factor FF%, d) Efficiency  $\eta$  %

#### 4.4.1. Front Contact Thickness

There are two layers in the front contact: the intrinsic ZnO layer and the Al-ZnO layer that makes up the window layer.

- The ZnO layer is resistive and serves to limit short-circuiting in areas where the CIGS is imperfectly covered by the buffer layer.
- The Al-ZnO layer enables the window layer to form the front contact part of the photovoltaic cell; it must be transparent to solar radiation, so that this radiation can be absorbed by the CIGS layer [28].

#### A) I-ZnO Insulating Layer Thickness

To study the effect of varying the thickness of the i-ZnO layer (ranging from 0.01  $\mu\text{m}$  to 0.1  $\mu\text{m}$ ), we set the value of the thickness of three combined layers (CIGS+p-Si+ $\text{In}_2\text{S}_3$ ) to 1.35  $\mu\text{m}$ , and then run the simulation to study the

efficiency of the cell's photovoltaic parameters. The results obtained are shown Fig (10). From the results obtained, it can be seen that changing the thickness of the i-ZnO layer does not affect the parameters of the photovoltaic cell.

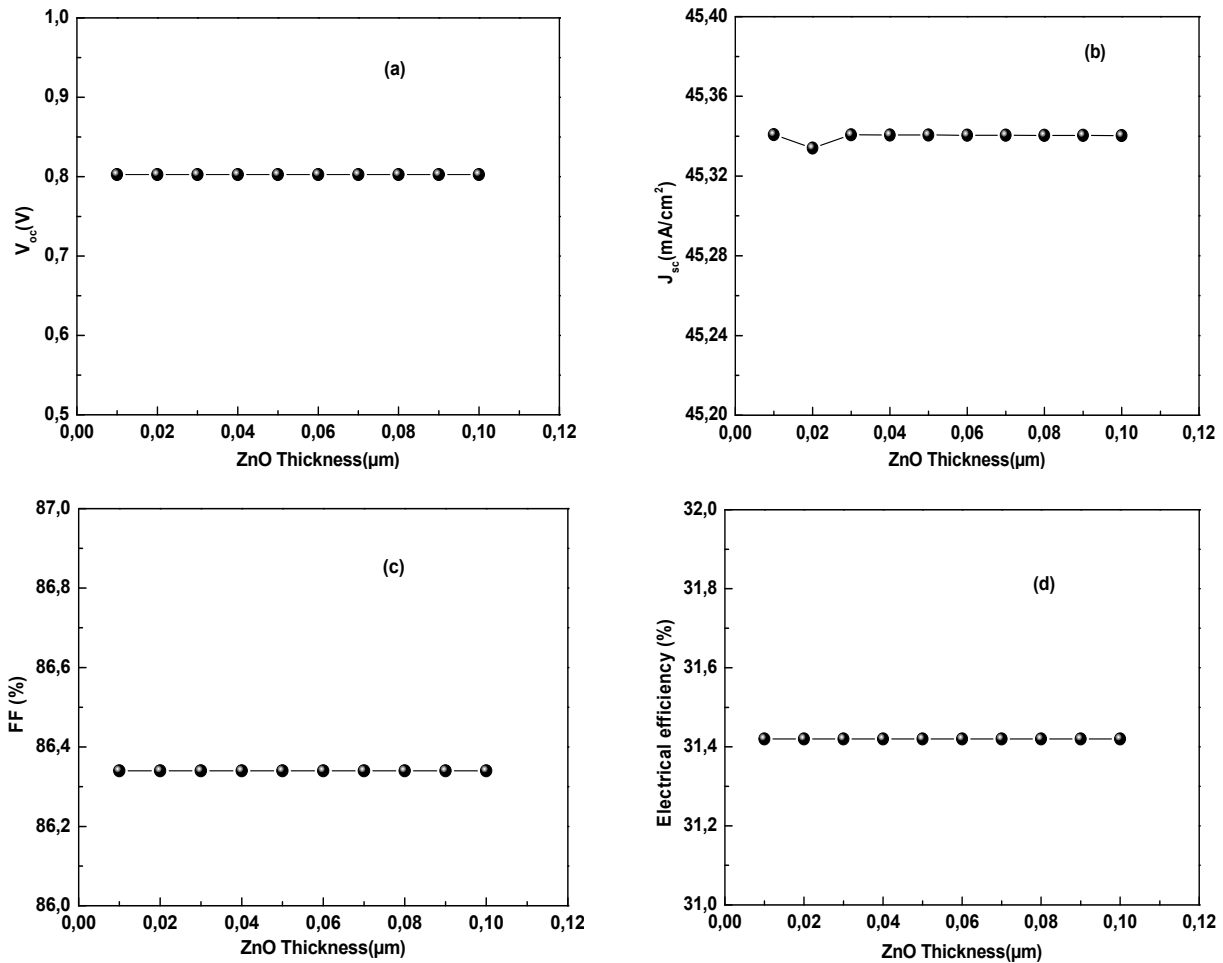


**Figure 10.** Effect of ZnO thickness on  
 a) The open-circuit voltage  $V_{oc}$ , b) The short-circuit current density  $J_{sc}$ , c) The form factor FF%, d) The efficiency  $\eta$  %

**b) Al-ZnO Window Layer Thickness**

To study the effect of varying the thickness of the Al-ZnO layer (ranging from 0.04 μm to 0.1 μm), we set the value of the thickness of four combined layers (CIGS+p-Si+ $In_2S_3$ +i-ZnO) to 1.42 μm, and then run the simulation to investigate the efficiency of the cell's photovoltaic parameters. The results obtained are shown in Fig. (11).

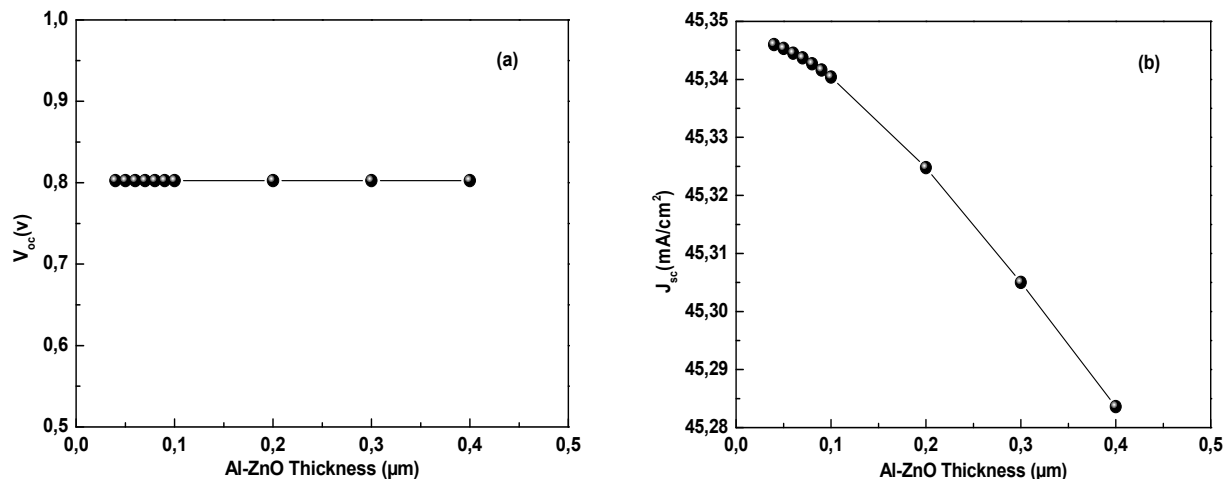


**Figure 11.** Effect of Al-ZnO thickness on  
 a) Open-circuit voltage  $V_{oc}$ , b) Short-circuit current density  $J_{sc}$ , c) Form factor FF%, d) Efficiency  $\eta$  %

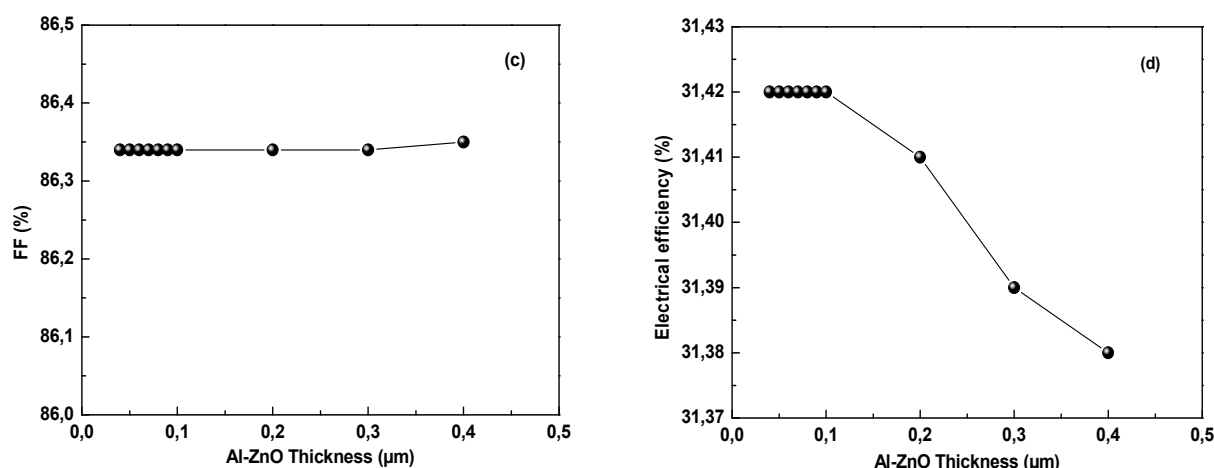


**Figure 11(continuation).** Effect of Al-ZnO thickness on

a) Open-circuit voltage  $V_{oc}$ , b) Short-circuit current density  $J_{sc}$ , c) Form factor FF%, d) Efficiency  $\eta$  %

From the results obtained, it can be seen that increasing the thickness of the Al-ZnO layer decreases the efficiency  $\eta$ . The range chosen for the Al-ZnO thickness has no influence on the short-circuit current density  $J_{sc}$ , the open-circuit voltage  $V_{oc}$  and the form factor FF. To improve cell efficiency, the Al-ZnO layer must be reduced. We therefore set the value of the Al-ZnO layer at  $0.1\ \mu\text{m}$ .

**Final results:** Table (7) shows the final results for the material parameter values used in our simulation.

**Table 7.** Final results for the material parameters used in our simulation.

Parameters	CIGS	P- Si	$\text{In}_2\text{S}_3$	I-Zno	Al-Zno
Thicknesses (nm)	0.3	0.8	0.05	0.07	0.1
Gap strip (eV)	1.300	1.0	2.800	3.200	3.400
Electronic affinity (eV)	4.500	4.500	4.700	4.600	4.600
Relative Permittivity	13.600	11.900	13.500	9.000	9.000
CB ( $1/\text{cm}^3$ )	2.200E +18	2.800E +19	1.800E +18	2.200E +18	2.200E +18
VB ( $1/\text{cm}^3$ )	1.800E +19	2.650E +19	4.000E +13	1.800E +19	1.800E +19
Electron mobility ( $\text{cm}^2/\text{Vs}$ )	1.000E +2	1.450E +3	4.000E +2	1.000E +2	1.000E +2
Hole mobility ( $\text{cm}^2/\text{Vs}$ )	2.500E +1	5.000E +2	2.100E +2	2.500E +1	2.500E +1
ND ( $1/\text{cm}^3$ )	0.000E +0	0.000E +0	1.000E +18	1.000E +16	1.000E +18
NA ( $1/\text{cm}^3$ )	2.000E +16	1.000E +20	1.000E +1	0.000E +0	0.000E +0
Defect density ( $1/\text{cm}^3$ )	1.000E +14	1.000E +14	1.000E +14	0.000E +0	0.000E +0

Based on these results, the photovoltaic parameter efficiencies found for the cell studied are shown in Table (8).

**Table 8.** Functional parameters of the CIGS solar cell.

$V_{oc}$ (V)	$J_{sc}$ ( $\text{mA}/\text{cm}^2$ )	FF (%)	$\eta$ (%)
0.1	0.8025	45.3404	31.42

## 5. CONCLUSION

Numerical simulation leads to a detailed understanding of how the structure of thin-film solar cells works. CIGS, a non-toxic material abundant on earth, is used in this study to analyze solar cell performance, bearing in mind that this material is expensive. To minimize the thickness of CIGS, the following solar cell structure was chosen: Al-ZnO/i-ZnO/ $\text{In}_2\text{S}_3$ /p-CIGS/p-Si. Where CIGS and Si are used as absorber layers and  $\text{In}_2\text{S}_3$  as buffer layer. The performance of CIGS-based solar cells was studied by varying the gap energy and thickness of each cell layer. Gap energy modifies solar cell performance. The gap energy of the absorber layers influences the cell's efficiency, while the other layers ( $\text{In}_2\text{S}_3$ , ZnO, Al-ZnO) do not have a great influence. Recombination rates influence the efficiency of the photovoltaic cell, reaching 26.12%. Increasing the thickness of the absorber layer has a major influence on efficiency, increasing it up to a certain limit. The best yield found after studying the variation in thickness of the total CIGS+p-Si absorber layer is 31.25%. The thicknesses of the CIGS, p-Si,  $\text{In}_2\text{S}_3$ , i-ZnO and Al-ZnO layers need to be in the order of  $0.3\ \mu\text{m}$ ,  $0.8\ \mu\text{m}$ ,  $0.05\ \mu\text{m}$ ,  $0.07\ \mu\text{m}$  and  $0.1\ \mu\text{m}$  respectively to achieve the best yield (31.42%). Finally, given the great complexity of increasing the conversion efficiency of solar cells and reducing their cost, many problems remain open for future investigation in order to fully understand the capabilities and limitations of the conversion efficiency of solar cells. We hope that the results presented in this work contribute to this understanding.

## ORCID

✉ D. Belfennache, <https://orcid.org/0000-0002-4908-6058>; ✉ Mohamed A. Ali, <https://orcid.org/0000-0002-7390-8592>

## REFERENCES

- [1] P. Bórawski, L. Holden, and A. Beldycka-Bórawska, *Energy*, **270**, 126804 (2023). <https://doi.org/10.1016/j.energy.2023.126804>
- [2] H. Sadamura, N. Suzuki, C. Sotome, et al. *Electrochemistry*, **78**(7), 594 (2010). <https://doi.org/10.5796/electrochemistry.78.594>
- [3] A. Jäger-Waldau, *Energies*, **13**(4), 930 (2020). <https://doi.org/10.3390/en13040930>
- [4] A. Jäger-Waldau, *PV Status Report*, (Publications Office of the European Union, Luxembourg, 2019). <https://doi.org/10.2760/326629, JRC118058>
- [5] M.A. Green, K. Emery, Y. Hishikawa, W. Warta, and E.D. Dunlop, *Progress in Photovoltaics: Research and Applications*, **23**, 1 (2015). <https://doi.org/10.1002/pip.2573>
- [6] D. Belfennache, D. Madi, R. Yekhlef, L. Toukal, N. Maouche, M.S. Akhtar, and S. Zahra, *Semicond. Phys. Quantum. Electron. Optoelectron.* **24**(4), 378 (2021). <https://doi.org/10.15407/spqeo24.04.378>
- [7] D. Belfennache, N. Brihi, and D. Madi, in: *Proceeding of the IEEE xplore, 8<sup>th</sup> (ICMIC) (2016)*, **7804164**, (2017), pp. 497–502. <https://doi.org/10.1109/ICMIC.2016.7804164>
- [8] R. Ouldamer, D. Madi, and D. Belfennache, in: *Advanced Computational Techniques for Renewable Energy Systems. IC-AIRES 2022. Lecture Notes in Networks and Systems*, vol. **591**, edited by M. Hatti, (Springer, Cham.2023). pp. 700-705, [https://doi.org/10.1007/978-3-031-21216-1\\_71](https://doi.org/10.1007/978-3-031-21216-1_71)
- [9] M. Zotti S. Mazzoleni, L.V. Mercaldo, M.D. Noce, M. Ferrara, P.D. Veneri, M. Diano, et al., *Heliyon*, **10**(4), e26323 (2024). <https://doi.org/10.1016/j.heliyon.2024.e26323>
- [10] D. Belfennache, D. Madi, N. Brihi, M.S. Aida, and M.A. Saeed, *Appl. Phys. A*, **124**, 697 (2018). <https://doi.org/10.1007/s00339-018-2118-z>
- [11] S.M. Govindharajulu, A.K. Jain, and M. Piraviperumal, *J. Alloys Compd.* **980**, 173588 (2024). <https://doi.org/10.1016/j.jallcom.2024.173588>
- [12] J. Raval, B. Shah, D. Kumar, S.H. Chaki, and M.P. Deshpande, *Chem. Eng. Sci.* **287**, 119728 (2024). <https://doi.org/10.1016/j.ces.2024.119728>
- [13] I. Repins, M. Contreras, B. Egaas, C. DeHart, J. Scharf, C. Perkins, B. To, and R. Noufi. *Progress in Photovoltaics: Research and Applications*, **16**(3), 235 (2008). <https://doi.org/10.1002/pip.822>
- [14] J. Lindahl, U. Zimmermann, P. Szaniawski, T. Törndahl, A. Hultqvist, P. Salomé, C. Platzer-Björkman, et al., *IEEE J. Photovolt.* **3**(3), 1100 (2013). <https://doi.org/10.1109/JPHOTOV.2013.2256232>
- [15] M. Powalla, P. Jackson, W. Witte, D. Hariskos, S. Paetel, C. Tschamber, and W. Wischmann, *Sol. Energy Mater. Sol. Cells*, **119**, 51 (2013). <https://doi.org/10.1016/j.solmat.2013.05.002>
- [16] A. Chirila, S. Buecheler, F. Pianezzi, P. Bloesch, C. Gretener, A.R. Uhl, C. Fella, et al., *Nature Mater*, **10**, 857 (2011). <https://doi.org/10.1038/nmat3122>
- [17] E. Wallin, U. Malm, T. Jarmar, O. Lundberg, M. Edoff, L. Stolt, et al., *Progress in Photovoltaics: Research and Applications*, **20**, 851 (2012). <https://doi.org/10.1002/pip.2246>
- [18] A. Romeo, M. Terheggen, D. Abou-Ras, D.L. Bätzner, F.-J. Haug, M. Kälin, D. Rudmann, et al., *Progress in Photovoltaics: Research and Applications*, **12**, 93 (2004). <https://doi.org/10.1002/pip.527>
- [19] M. Kemell, M. Ritala, and M. Leskelä, *Crit. Rev. Solid State Mater. Sci.* **30**, 1 (2005). <https://doi.org/10.1080/10408430590918341>
- [20] C.H. Fischer, M. Bär, T. Glatzel, I. Lauermaun, and M.C. Lux-Steiner, *Sol. Energy Mater. Sol. Cells*, **90**(10), 1471 (2006). <https://doi.org/10.1016/j.solmat.2005.10.012>
- [21] K.S. Ramaiah, and V.S. Raja, *Sol. Energy Mater. Sol. Cells*, **32**, 1 (1994). [https://doi.org/10.1016/0927-0248\(94\)90250-X](https://doi.org/10.1016/0927-0248(94)90250-X)
- [22] M. Burgelman, P. Nollet, and S. Degraeve, *Thin Solid Films*, **361-362**, 527 (2000). [https://doi.org/10.1016/S0040-6090\(99\)00825-1](https://doi.org/10.1016/S0040-6090(99)00825-1)
- [23] K. Decock, S. Khelifi, and M. Burgelman, *Thin Solid Films*, **519**(21), 7481 (2011). <https://doi.org/10.1016/j.tsf.2010.12.039>
- [24] M. Burgelman, and J. Marlein, Analysis of graded band gap solar cells with SCAPS, In: *Proceedings of the 23<sup>rd</sup> European photovoltaic solar energy conference*, (2008). pp. 2151-2156.
- [25] J. Verschraegen, and M. Burgelman, *Thin Solid Films*, **515**(15), 6276 (2007). <https://doi.org/10.1016/j.tsf.2006.12.049>
- [26] S. Degraeve, M. Burgelman, and P. Nollet, in: *Proceedings of the 3<sup>rd</sup> world conference on photovoltaic energy conversion*, (2003), pp. 487-490. <http://hdl.handle.net/1854/LU-404099>
- [27] A. Niemegeers, and M. Burgelman, in: *Proceedings of the 25<sup>th</sup> IEEE photovoltaic specialists conference*, 901e4 (1996). <https://doi.org/10.1109/PVSC.1996.564274>
- [28] R.N. Mohottige, and S.P.K. Vithanage, *J. Photochem. Photobiol. A: Chem.* **407**, 113079 (2021). <https://doi.org/10.1016/j.jphotochem.2020.113079>
- [29] M. Mostefaoui, H. Mazan, S. Khelifi, A. Bouraiou, and R. Dabou, *Energy Procedia*, **74**, 736 (2015). <https://doi.org/10.1016/j.egypro.2015.07.809>
- [30] K. Orgassa, H.W. Schock, and J.H. Werner, *Thin Solid Films*, **431-432**, 387 (2003). [https://doi.org/10.1016/S0040-6090\(03\)00257-8](https://doi.org/10.1016/S0040-6090(03)00257-8)
- [31] M. Hashemi, Z. Saki, M. Dehghani, F. Tajabadi, S.M.B. Ghorashi, and N. Taghavinia, *Sci. Rep.* **12**, 14715 (2022). <https://doi.org/10.1038/s41598-022-18579-w>
- [32] R.J. Matson, O. Jamjoum, A.D. Buonaquisti, P.E. Russell, L.L. Kazmerski, P. Sheldon, and R.K. Ahrenkiel, *Solar cells*, **11**(3), 301 (1984). [https://doi.org/10.1016/0379-6787\(84\)90019-X](https://doi.org/10.1016/0379-6787(84)90019-X)
- [33] N. Kohara, S. Nishiwaki, Y. Hashimoto, T. Negami, T. Wada, *Sol. Energy Mater. Sol. Cells*, **67**(1-4), 209 (2001). [https://doi.org/10.1016/S0927-0248\(00\)00283-X](https://doi.org/10.1016/S0927-0248(00)00283-X)
- [34] M. Powalla, and B. Dimmler, *Thin Solid Films*, **361-362**, 540 (2000). [https://doi.org/10.1016/S0040-6090\(99\)00849-4](https://doi.org/10.1016/S0040-6090(99)00849-4)
- [35] C.K.G. Kwok, H. Tangara, N. Masuko, et al., *Sol. Energy Mater. Sol. Cells*, **269**, 112767 (2024). <https://doi.org/10.1016/j.solmat.2024.112767>

- [36] S. Mahdid, D. Belfennache, and D. Madi, *et al.*, J. Ovonic. Res. **19**(5), 535 (2023). <https://doi.org/10.15251/JOR.2023.195.535>
- [37] R. Ouldamer, D. Belfennache, D. Madi, *et al.*, J. Ovonic. Res. **20**(1), 45 (2024). <https://doi.org/10.15251/JOR.2024.201.45>

### ЧИСЕЛЬНЕ МОДЕЛЮВАННЯ ПІДВИЩЕННЯ ЕЛЕКТРИЧНОЇ ЕФЕКТИВНОСТІ СОНЯЧНОГО ЕЛЕМЕНТУ НА ОСНОВІ CIGS НА SCAPS-1D

К. Мадуй<sup>а</sup>, А. Гечі<sup>б</sup>, С. Мадуй<sup>с</sup>, Р. Єхлеф<sup>д</sup>, Д. Бельфенаше<sup>д</sup>, С. Зайїу<sup>е,ф</sup>, Мохамед А. Алі<sup>г</sup>

<sup>а</sup>Лабораторія прикладної оптики Інституту оптики і точної механіки університет Ферхат АББАС Сетіф-16 Алжир

<sup>б</sup>Лабораторія оптоелектроніки та компонентів, інститут оптики і точної механіки, університет Ферхат Аббас Сетіф, Алжир

<sup>с</sup>Лабораторія прикладної біохімії, Університет Ферхат Аббас Сетіф-1, 19000, Алжир

<sup>д</sup>Науково-дослідний центр промислових технологій CRTI, P.O. Box 64, Черага, 16014, м. Алжир, Алжир

<sup>е</sup>Лабораторія досліджень поверхонь і розділів твердих матеріалів (LESIMS), Університет Сетіф 1, 19000 Сетіф, Алжир

<sup>ф</sup>Факультет природничих наук і життя, Університет Сетіф-1, 19000 Сетіф, Алжир

<sup>г</sup>Школа біотехнології, Університет Бадр в Каїрі (BUC), Бадр сіті, 11829, Каїр, Єгипет

Сонячні елементи в даний час знаходяться в центрі великої кількості досліджень. Мета – знизити їх собівартість. Щоб досягти цього, нам потрібно зменшити масу матеріалів і підвищити ефективність перетворення цих сонячних елементів. Це спонукало до дослідження використання тонких плівок, таких як a-Si, CdTe, CIGS. Це підвищення ефективності вимагає оптимізації параметрів фотоелектричної системи. У цьому моделюванні та імітаційній роботі ми використовуємо програмне забезпечення SCAPS-1D для вивчення впливу швидкості рекомбінації електронів і дірок у шарі CIGS, впливу товщини шарів і впливу енергії розриву кожного шару. матеріалу, використаного для цієї сонячної батареї, на струм короткого замикання  $J_{sc}$ , напругу холостого ходу  $V_{oc}$ , форм-фактор FF та електричний ККД  $\eta$  елементу CIGS для Mo/p-CIGS/p-Si/In<sub>2</sub>S<sub>3</sub>/одноперехідної структури i-ZnO/Al-ZnO. У цьому дослідженні ми виявлено, що швидкість рекомбінації впливає на ефективність фотоелектричного елемента. Енергія проміжку шарів поглинача впливає на ефективність елемента, тоді як інші шари (In<sub>2</sub>S<sub>3</sub>, ZnO, Al-ZnO) не мають великого впливу на продуктивність сонячного елемента, а збільшення товщини шару поглинача має великий вплив на ефективність, збільшивши його до певної межі. Товщина шарів CIGS, p-Si, In<sub>2</sub>S<sub>3</sub>, i-ZnO та Al ZnO має бути порядку 0,3 мкм, 0,8 мкм, 0,05 мкм, 0,07 мкм та 0,1 мкм відповідно для досягнення кращої ефективності (31,42%).

**Ключові слова:** теорія функціоналу густини (DFT); енергія зв'язку; гомо-люмо енергія; енергія фрагментації; магнітний момент